THE JOURNAL OF PHYSICAL CHEMISTRY B

Article

pubs.acs.org/JPCB

Self-Assembly of a Mixture System Containing Polypeptide Graft and Block Copolymers: Experimental Studies and Self-Consistent Field Theory Simulations

Zeliang Zhuang, Xiaomeng Zhu, Chunhua Cai, Jiaping Lin,* and Liquan Wang

Shanghai Key Laboratory of Advanced Polymeric Materials, State Key Laboratory of Bioreactor Engineering, Key Laboratory for Ultrafine Materials of Ministry of Education, School of Materials Science and Engineering, East China University of Science and Technology, Shanghai 200237, China

Supporting Information

ABSTRACT: Self-assembly behavior of mixture systems containing poly(γ-benzyl-L-glutamate)−poly(ethylene glycol) graft (PBLG-*g*-PEG) and block (PBLG-*b*-PEG) copolymers in aqueous solution was investigated by both experiments and computer simulations. Pure graft copolymers self-assembled into vesicles, and pure block copolymers aggregated into spherical micelles or vesicles, while, for the mixture systems, hybrid cylindrical micelles were observed. In addition to the experimental observations, self-consistent field theory (SCFT) simulations were performed on the self-assembly behavior of graft/block copolymer mixtures. Simulation results reproduced the morphological transitions observed in the experiments. Moreover, from the SCFT simulations, the chain distributions of copolymers in the aggregates were obtained. For the hybrid cylindrical micelles, block copolymers were found to mainly locate at the ends of aggregates, which prevents the fusion of cylinders to vesicles. By combining experimental findings with simulation results, the mechanism regarding the morphological transition of the aggregates formed by graft/block copolymer mixtures is proposed.

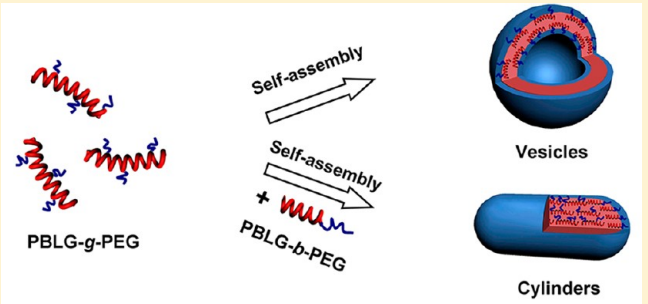

Self-assembly of polypeptide graft/block copolymer mixtures

INTRODUCTION

Amphiphilic block and graft copolymers have been found to self-assemble into nanosized supramolecular aggregates in selective solvents. Diversiform morphologies, such as spheres, rods, vesicles, spindles, tubules, toroids, and other complex structures have been observed.[1−6] These structures have attracted widespread interest for their potential applications in drug delivery systems, coatings, cosmetics, and nanoreactors.[7,8] To facilitate their practical applications, it is important to make these self-assembled structures with controllable shapes and size, as well as specific functions.[9−11]

Cooperative self-assembly of two copolymers has been proved to be a promising strategy to obtain aggregates with controllable morphologies and structures.[12−16] For example, Eisenberg et al. prepared hybrid vesicles from a mixture of polystyrene-*b*-poly(acrylic acid) (PS-*b*-PAA) and polystyrene-*b*-poly(4-vinylpyridine) (PS-*b*-P4VP). The structures of these hybrid vesicles can be tailored by changing the lengths of PAA and P4VP blocks.[12] The molecular architecture of copolymers is an important factor determining aggregate structures and properties. In comparison with simple diblock copolymers, nonlinear copolymers, such as graft and star-like copolymers, could display more sophisticated self-assembly behavior.[17−22] So far, limited attention has been devoted to the mixture systems consisting of nonlinear copolymers; however, interesting phenomena have been observed.[23−25] A representive example reported by Lodge's group is that hamburger-like micelles with a narrow size distribution were obtained via cooperative self-assembly of star-like terpolymers and linear block copolymers.[25] Among these nonlinear copolymers, graft copolymers show advantages in altering the side chain properties by using a convenient grafting strategy, which facilitates the fabrication of self-assembled aggregates with multiple morphologies and functions.[26−29] It is anticipated that controllable property of self-assembled hybrid structures from mixtures containing graft copolymers can be obtained.

Recently, increasing attention has been paid to polypeptide-based self-assemblies due to their biocompatibility and advantages in controlling both the functions and structures of the supramolecular aggregates.[30−35] Co-assembly of polypeptide-based copolymer mixtures is a particular potential approach to creating novel supramolecular structures.[36−38] For example, our group reported that poly(γ-benzyl-L-glutamate)-*b*-poly(ethylene glycol) (PBLG-*b*-PEG) block copolymers and PBLG homopolymers can cooperatively self-assemble into complex superhelices with uniform diameter and screw-pitch.[37] In addition, polypeptide-based graft copolymers are another important building block to prepare abundant self-

Received: June 17, 2012
Revised: July 27, 2012
Published: July 27, 2012

dx.doi.org/10.1021/jp305956v | J. Phys. Chem. B 2012, 116, 10125−10134

assembly structures.[28,34,39] However, there are few works concerning the self-assembly behavior of mixture systems containing polypeptide-based graft copolymers.[40,41] Meanwhile, the mechanism underlying the self-assembly of polypeptide mixtures is still not clear enough. Thus, studies on the self-assembly behavior of such mixture systems could be helpful for knowing the aggregation behavior of complex polypeptides and, by extension, protein systems.

Experimentally understanding the self-assembly behavior of copolymers usually suffers from difficulties arisen from limited experimental techniques. Computer simulation, such as self-consistent field theory (SCFT), has been proven to be a powerful tool to investigate the self-assembly of amphiphilic block copolymers.[42−45] Recent research has confirmed that the simulations not only support the experimental results, but also provide valuable information that can not be discerned using currently available experimental techniques.[46−48] For instance, Jiang et al. investigated the self-assembly behavior of a linear amphiphilic ABC triblock copolymer by both experiments and SCFT simulations, and multicompartment micelles with bump-surface were observed.[46] In addition, SCFT simulations have been extended to investigate the self-assembly behavior of mixture systems in solutions.[49−51] Yang's group simulated the micellization of amphiphilic ABC star triblock copolymers and the mixtures with their counterpart linear AB diblock copolymers. It was found that the simulation results were in good agreement with existing experimental findings.[49] These researches show that combining the experimental and simulation studies is an effective strategy to investigate the self-assembly process of mixture systems.

In this work, the self-assembly behavior of mixture systems comprising poly(γ-benzyl-L-glutamate)−poly(ethylene glycol) graft (PBLG-*g*-PEG) and block (PBLG-*b*-PEG) copolymers was investigated. It was found that pure graft copolymers self-assembled into vesicles, and pure block copolymers aggregated into spherical micelles or vesicles. For the mixtures, cylindrical micelles were obtained. In addition to experimental studies, SCFT simulations on the self-assembly of the graft/block copolymer mixtures were performed to further verify the aggregate structures and provide chain density distributions in the aggregates. By combining experimental findings with SCFT results, the mechanism regarding the morphological transition of the graft/block copolymer mixtures is proposed.

EXPERIMENTAL SECTION

Materials. Methoxypolyethylene glycol amine (mPEG−NH_2) (M_w = 750) and polyethylene glycol monomethyl ether (mPEG−OH) (M_w = 750) were purchased from Sigma Inc. The dialysis bag (Membra-cel, 3500 molecular weight cutoff) was provided by Serva Electrophoresis GmbH. Analytical-grade hexane, tetrahydrofuran (THF), and 1,4-dioxane were refluxed with sodium and distilled immediately before use. All the other regents were of analytical grade and used as received.

Synthesis of PBLG Homopolymer and PBLG-*g*-PEG Graft Copolymer. γ-Benzyl-L-glutamate-*N*-carboxyanhydride (BLG-NCA) was synthesized according to the literature procedure.[52] PBLG was obtained by ring-opening polymerization of BLG-NCA initiated by triethylamine with 1,4-dioxane as solvent.[52,53] After 3 days, the viscous reaction mixture was poured into a large volume of anhydrous ethanol. The precipitated product was dried under vacuum and then purified twice by repeated precipitation from a chloroform solution into a large volume of anhydrous methanol. The molecular weight of the PBLG homopolymer is estimated to be 171 000 from the intrinsic viscosity ([η]) value measured in dichloroacetic acid. The gel permeation chromatography (GPC) analysis (Waters 1515, DMF as eluent solvent) showed that the molecular weight distribution of the PBLG homopolymer is 1.18.

PBLG-*g*-PEG graft copolymers (abbreviated as GP, see Scheme 1a) were prepared by ester exchange reaction of PBLG

Scheme 1. Molecular Structures of (a) PBLG-*g*-PEG Graft Copolymer and (b) PBLG-*b*-PEG Block Copolymer

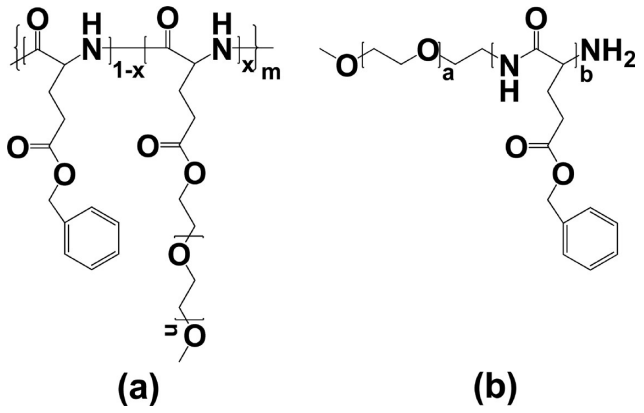

homopolymer with mPEG−OH.[39,40,54] The feed molar ratio of mPEG−OH to BLG units is 0.05, and the reaction was performed at 55 °C for 1.5 h in 1,2-dichloroethane with *p*-toluenesulfuric acid as a catalyst. Then the reaction mixture was precipitated into a large volume of anhydrous methanol. The product was purified twice by repeated precipitation from a chloroform solution into a large volume of anhydrous methanol and dried under vacuum. The degree of grafting of GP is defined as the ratio of the number of PEG chains to the total degree of polymerization of the polypeptide backbone, which can be calculated from the peak intensities of the methylene proton signal (5.1 ppm) of PBLG and the ethylene proton signal (3.6 ppm) of PEG in the ^{1}H NMR spectrum. Calculation showed that the average number of PEG side chain in per PBLG backbone is 4.3, and the degree of grafting is 0.55%. The volume fraction of PEG for the graft copolymers is 0.02.

Synthesis of PBLG-*b*-PEG Block Copolymers. PBLG-*b*-PEG block copolymers (abbreviated as BP, see Scheme 1b) were synthesized by ring-opening polymerization of BLG-NCA initiated by mPEG-NH_2.[53] Two block copolymers, $PBLG_{28000}$-*b*-PEG_{750} (BP1) and $PBLG_{5500}$-*b*-PEG_{750} (BP2), were synthesized. The subscripts denote the molecular weights for each block. The molecular weights of the block copolymers were calculated from the polymer compositions, which are determined by the ^{1}H NMR spectrum. GPC analysis showed that the molecular weight distributions of BP1 and BP2 are 1.22 and 1.20, respectively. The volume fractions of PEG for BP1 and BP2 are 0.03 and 0.13, respectively.

Preparation of Micelles. The polymeric micelle solutions were prepared using a dialysis method. First, PBLG-*g*-PEG graft copolymers and PBLG-*b*-PEG block copolymers were separately dissolved in THF with a polymer concentration of 0.25 g/L. Then the GP and BP solutions were mixed together with various volume ratios and stirred for 2 days to obtain homogeneous solutions. To prepare the micelle solution, 2.5 mL of deionized water was added to 10 mL of a GP/BP mixture stock solution at a rate of 0.02 mL/s with vigorous

dx.doi.org/10.1021/jp305956v | J. Phys. Chem. B 2012, 116, 10125−10134

stirring. Subsequently, the solution was dialyzed against deionized water for 3 days to remove the organic solvents. Before analysis, the solutions were stabilized for at least 5 days.

Transmission Electron Microscopy (TEM). The morphologies of the aggregates were examined by TEM (H-800, HITACHI) operated at an accelerating voltage of 200 kV. Drops of solution were placed on a copper grid coated with carbon film and then were dried at room temperature.

Scanning Electron Microscopy (SEM). The morphologies of the aggregates were also observed by SEM (S4800, HITACHI) operated at an accelerating voltage of 15 kV. The samples were prepared by placing drops of solution on a copper grid coated with carbon film and then were dried at room temperature. Before the observations, the samples were sputtered by Aurum.

Atomic Force Microscopy (AFM). AFM measurements were performed with an XE-100 (Park Systems) by using the noncontact mode at room temperature in air. The samples were prepared by placing drops of solution on a freshly cleaved mica surface and allowed to dry in air.

Laser Light Scattering (LLS) Measurements. LLS was measured by an LLS spectrometer (ALV/CGS-5022F) equipped with an ALV-High QE APD detector and an ALV-5000 digital correlator using a He−Ne laser (the wavelength λ = 632.8 nm) as the light source. All the samples were filtered through 0.8 μm filters, and the measurements were carried out at 20 °C.

In static LLS, the angular dependence of the excess absolute time-average scattered intensity, i.e. Rayleigh ratio $R_{vv}(q)$ of the dilute polymer solutions was measured. $R_{vv}(q)$ is related to the weight-average molar mass (M_w), polymer concentration (C), and the scattering angle (φ) as

$$KC/R(\varphi, C) = 1/M_w[1 + (R_g{}^2q^2)/3]c + 2A_2C \quad (1)$$

where $K = 4\pi^2n^2(dn/dC)^2/(N_A\lambda^4)$ and $q = 4\pi n \sin(\varphi/2)/\lambda$ with N_A, dn/dC, n, and λ being the Avogadro number, the specific refractive index increment, the solvent refractive index, and the wavelength of the light in vacuum, respectively; A_2 is the second virial coefficient, and R_g is the z-average radius of gyration of the aggregates in solution. By extrapolating to zero concentration and zero angle, R_g values of the aggregates can be calculated.

In dynamic LLS measurement, the Laplace inversion of each measured intensity−intensity time correlation function $G^{(2)}(t,q)$ in the self-beating mode can result in a line width distribution $G(\Gamma)$. The translational diffusion coefficient D calculated from the decay time, Γ, by the slope of the Γ versus q^2 plot, can lead to hydrodynamic radius R_h by the Stokes−Einstein equation $R_h = k_BT/(6\pi\eta D)$, where k_B, T, and η are the Boltzmann constant, the absolute temperature, and the solvent viscosity, respectively.

SCFT for Mixtures of Graft and Block Copolymers in Solution. A system with volume V, consisting of n_1 AB graft copolymers, n_2 AB block copolymers, and n_S solvent molecules were considered. Each AB graft copolymer is composed of one homopolymer A backbone and m homopolymer B grafts. The degrees of polymerization of the A backbone and every B graft are N_{A1} and N_{B1}, and the total number of blocks, N_g, is equal to $N_{A1} + mN_{B1}$. For AB block copolymers, the total number of blocks N_b is equal to $N_{A2} + N_{B2}$. The number-average chain length of the polymer mixtures, $\bar{N} = N_gP_{N_g} + N_bP_{N_b}$, is used as the reference chain length, where P_{N_g} and P_{N_b} are the number percentage of different chain lengths for N_g and N_b, respectively. Accordingly, the volume fractions of A blocks in graft and block copolymers are f_{A1} and f_{A2}, respectively, and those of B blocks are f_{B1} and f_{B2}, respectively ($f_{A1}+f_{B1} = 1, f_{A2} + f_{B2} = 1$). The A and B blocks are assumed to be incompressible and have a common volume ρ_0^{-1}. The volume fractions of graft copolymers, block copolymers, and solvents are c_g, c_b, and c_S, respectively, and the total volume fraction of the copolymer mixtures is $c_P = c_g + c_b = 1 - c_S$, and was fixed to be $c_P = 0.1$ in the present simulation. ν_b is defined as the volume ratio of block copolymer to total graft/block copolymers. Thus, $c_b = c_P\nu_b$ and $c_g = c_P(1 - \nu_b)$. Herein, the position of ith graft is given by τ_i, which is distributed at the A backbone with uniform interval. Furthermore, we assume that the A and B blocks have the same statistical length a.

Within the SCFT, the pair interactions between the different components are determined by a set of effect chemical potential fields ω_K (K = A, B, S), replacing actual interactions in solution. Thus, the free energy (in units of k_BT) of the graft/block copolymer systems in solution is given by[50,55]

$$F = -c_g\ln(Q_g/V) - c_b\ln(Q_b/V) - Nc_S\ln(Q_S/V) + 1/V\int dr\left[\frac{1}{2}\sum_{\substack{i,j=A,B,S\\ i\neq j}} x_{ij}\bar{N}\phi_i\phi_j - \sum_{i=A,B,S} w_i\phi_i - \xi\left(1 - \sum_{i=A,B,S}\phi_i\right)\right] \quad (2)$$

where χ_{ij} is the Flory−Huggins interaction parameter between species i and j. The density fields, ϕ_A, ϕ_B, and ϕ_S, represent the local volume fractions of A block, B block, and solvent, respectively. ξ is the Lagrange multiplier, invoked by incompressibility condition ($\sum_{i=A,B,S}\phi_i = 1$). Then, $Q_g = \int d\mathbf{r}q_{A1}(\mathbf{r}, N_g)$ and $Q_b = \int d\mathbf{r}q_{A2}(\mathbf{r}, N_b)$ are the partition functions for a single graft copolymer chain and a single block copolymer chain in the effective chemical potential fields w_A and w_B. Additionally, Q_S is the partition function of a solvent molecule in the fields w_S given by $Q_S = \int d\mathbf{r}\exp(-w_S(\mathbf{r})/\bar{N})$. The propagator $q(\mathbf{r},s)$, which represents the probability of finding blocks s at position $\mathbf{r}$, is the fundamental quantity to be calculated in mean-field studies. It satisfies a modified diffusion equation using a flexible Gaussian chain model. The minimization of free energy F, with respect to $\phi_A(\mathbf{r})$, $\phi_B(\mathbf{r})$, $\phi_S(\mathbf{r})$, and $\zeta(\mathbf{r})$, can lead to a set of mean-field equations describing the thermodynamic behavior of copolymers:

$$\phi_A = \frac{Vc_gf_{A1}}{Q_gN_{A1}}\sum_{i=1}^{m+1}\int_{\tau_{i-1}N_{A1}}^{\tau_iN_{A1}} dsq_{A1}(\mathbf{r}, s)q_{A1}^+(\mathbf{r}, s) + \frac{Vc_bf_{A2}}{Q_bN_{A2}}\int_0^{N_{A2}} dsq_{A2}(\mathbf{r}, s)q_{A2}^+(\mathbf{r}, s) \quad (3)$$

dx.doi.org/10.1021/jp305956v | J. Phys. Chem. B 2012, 116, 10125−10134

$$\phi_B = \frac{Vc_g f_{B1}}{mQ_g N_{B1}} \sum_{j=1}^{m} \int_0^{N_{B1}} ds q_{B1}(\mathbf{r}, s) q_{B1j}^{+}(\mathbf{r}, s) + \frac{Vc_b f_{B2}}{Q_b N_{B2}} \int_0^{N_{B2}} ds q_{B2}(\mathbf{r}, s) q_{B2}^{+}(\mathbf{r}, s) \quad (4)$$

$$\phi_S = \frac{f_S V}{Q_S} \exp(-w_S(\mathbf{r})/\bar{N}) \quad (5)$$

$$w_A = \chi_{AB}\bar{N}\phi_B(\mathbf{r}) + \chi_{AS}\bar{N}\phi_S(\mathbf{r}) + \xi(\mathbf{r}) \quad (6)$$

$$w_B = \chi_{AB}\bar{N}\phi_A(\mathbf{r}) + \chi_{BS}\bar{N}\phi_S(\mathbf{r}) + \xi(\mathbf{r}) \quad (7)$$

$$w_S = \chi_{AS}\bar{N}\phi_A(\mathbf{r}) + \chi_{BS}\bar{N}\phi_B(\mathbf{r}) + \xi(\mathbf{r}) \quad (8)$$

$$\phi_A(\mathbf{r}) + \phi_B(\mathbf{r}) + \phi_S(\mathbf{r}) = 1 \quad (9)$$

The details about the numerical calculation of SCFT can be found in our previous work.[56] The simulations were carried out in two dimensions on a 128 × 128 lattice with periodic boundary conditions. The counter step size was set to be 0.01. The numerical simulation was carried out until the relative free energy changes at each iteration were smaller than 10^{-5} and the incompressibility condition was achieved. The same initial density fluctuation amplitude was used in our simulations to ensure that the resulting aggregate morphologies were not affected by the initial density fluctuation. Furthermore, the simulation was repeated 10−20 times by starting with different initial random states and different random numbers to guarantee that the observed morphologies were not accidental.

In the simulations, the parameters were chosen as follows. For the graft copolymers, the volume fraction of the A block f_{A1}, the number of B block branches m, and the position of first junction point τ were set as f_{A1} = 0.75, m = 3, and τ = 0.1, respectively. For the block copolymers, the volume fraction of the A block was set as f_{A2} = 0.78. The Flory−Huggins parameters were set as χ_{AB} = 0.5, χ_{AS} = 7.5, and χ_{BS} = 0. The length of a single graft copolymer chain N_g and that of single block copolymer chain N_b were assumed to be N_g = 55 and N_b = 20, which describes the case where the molecular weight of graft copolymer is higher than that of block copolymer.

RESULTS AND DISCUSSION

Morphologies of Aggregates Self-Assembled from Mixture Systems. When selective solvent (water) was added to PBLG-*g*-PEG/PBLG-*b*-PEG (GP/BP) stock solution, the hydrophobic polypeptide blocks become insoluble and tended to form aggregate core outspread with hydrophilic PEG chains. Figure 1 shows typical TEM images of the aggregate morphologies self-assembled from PBLG-*g*-PEG/PBLG$_{28000}$-*b*-PEG$_{750}$ (GP/BP1) mixtures with various weight fraction of BP1, m_{BP1}, which is defined as the ratio of the weight of BP1 to the total weight of BP1 and GP. For the pure graft copolymers, as shown in Figure 1a, vesicles with an average diameter of 300 nm were obtained, which is consistent with our previous work.[39] Pure BP1 block copolymers also aggregate into vesicles (Figure 1b). For the mixtures, cylindrical micelles are always observed. As shown in Figure 1c−e, with increasing m_{BP1}, both the length and diameter of cylinders decrease. In addition, the structure of the aggregates can be affected by many factors, such as initial solvent nature, initial polymer concentrations, and the adding rate of selective solvent.[39] For example, we found that

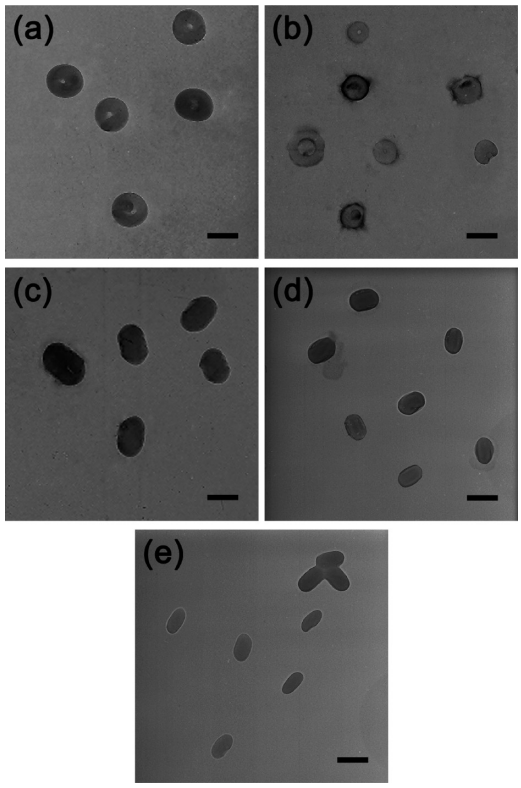

Figure 1. TEM images of the aggregates self-assembled from GP/BP1 mixtures with various weight fractions of BP1 (m_{BP1}): (a) 0, (b) 1, (c) 0.25, (d) 0.5, and (e) 0.75. The scale bars represent 300 nm.

the size of vesicles, cylinders, and spheres self-assembled from mixture systems decreases by increasing the adding rate of water and diluting the initial polymer concentration. Since the major concern of the present work is to understand the effect of mixing on the self-assembly, we did not consider these affecting factors.

When a spherical micelle-forming (Figure 2a) block copolymer PBLG$_{5500}$-*b*-PEG$_{750}$ (BP2) bearing a shorter PBLG chain was used, cylindrical micelles were also obtained from

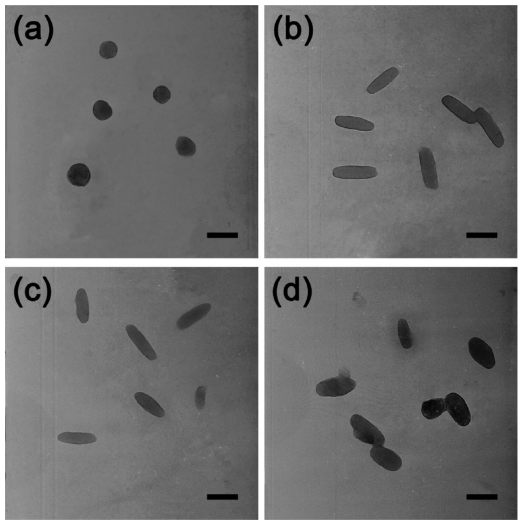

Figure 2. TEM images of the aggregates self-assembled from GP/BP2 mixtures with various weight fractions of BP2 (m_{BP2}): (a) 1, (b) 0.25, (c) 0.5, and (d) 0.75. The scale bars represent 300 nm.

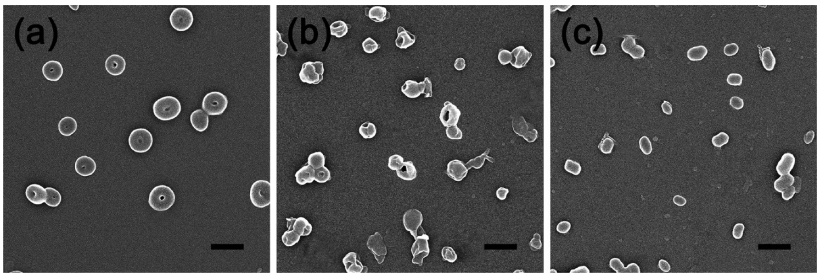

Figure 3. SEM images of the aggregates self-assembled from (a) GP, (b) BP1, and (c) GP/BP1 mixture (m_{BP1} = 0.5). The scale bars represent 500 nm.

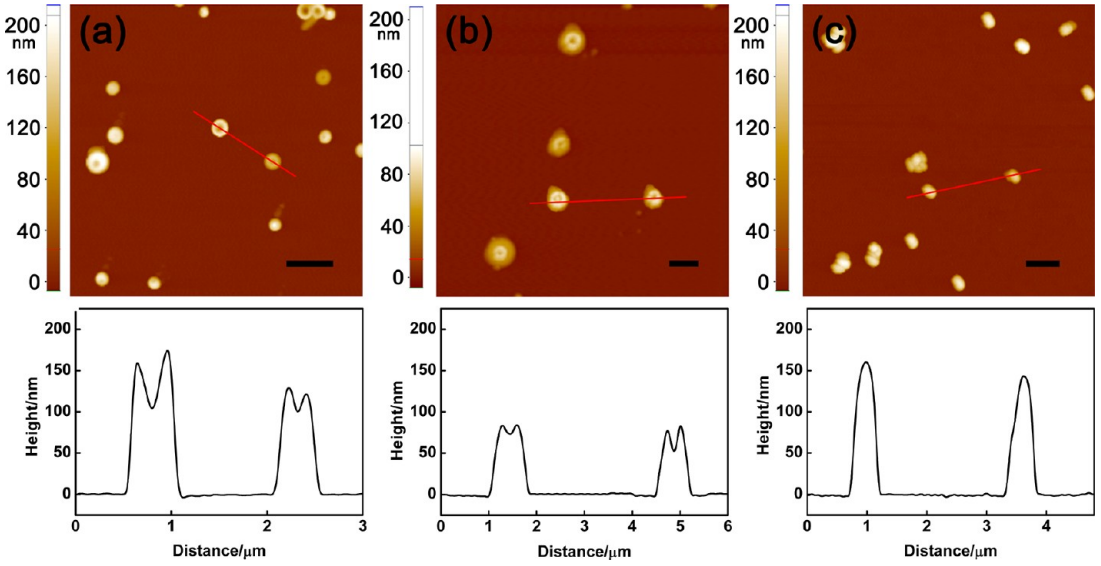

Figure 4. AFM images of the aggregates self-assembled from (a) GP, (b) BP1, and (c) GP/BP1 mixture (m_{BP1} = 0.5). The scale bars represent 1 μm.

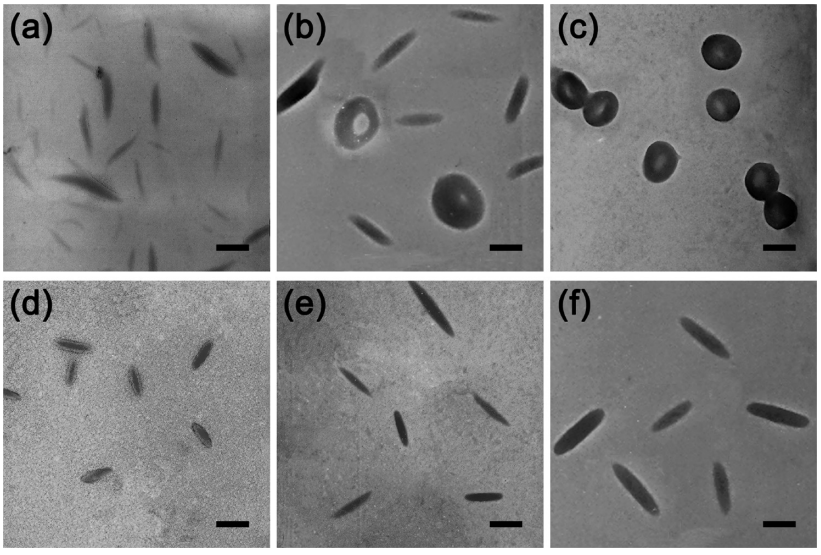

Figure 5. TEM images of the aggregates self-assembled from GP/BP2 mixtures with various added water contents: (a) 5, (b) 15 and (c) 25 vol % at m_{BP2} = 0; and (d) 5, (e) 15, and (f) 25 vol % at m_{BP2} = 0.5. The scale bars represent 300 nm.

GP/BP2 mixtures. As shown in Figure 2b–d, with increasing the weight fraction of BP2 in the mixtures (m_{BP2}), the length of cylinders slightly decreases. Furthermore, when a less asymmetric block copolymer, $PBLG_{11000}$-*b*-PEG_{5000}, was used, cylindrical micelles were also self-assembled from the PBLG-*g*-PEG/$PBLG_{11000}$-*b*-PEG_{5000} mixture system. The above observations indicate that the self-assembly behavior of PBLG-*g*-PEG graft copolymers is dramatically changed by introducing PBLG-*b*-PEG block copolymers.

The aggregate morphologies were further examined by SEM and AFM analyses. Shown in Figure 3 are typical SEM images of the aggregates from GP, BP1 and their mixture with equal

dx.doi.org/10.1021/jp305956v | J. Phys. Chem. B 2012, 116, 10125–10134

weight (m_{BP1} = 0.5). As shown in Figure 3a,b, both the vesicles formed by pure GP and BP1 are in spherical shape but collapse and show a lower center on the surface of the aggregates. For the aggregates self-assembled from mixtures, cylindrical images were observed (Figure 3c). Figure 4 represents the AFM results for these aggregates. As can be seen, the AFM images of both GP and BP1 vesicles display higher periphery and lower center (Figure 4a and 4b), which is a typical image for vesicles.[57] Figure 4c shows the AFM image of solid cylindrical structure of the aggregates self-assembled from the mixtures. In addition, SEM images of the aggregates self-assembled from GP/BP1 mixtures with other compositions (m_{BP1} = 0.25, and 0.75), as well as GP/BP2 mixtures are provided in the Supporting Information (Figures S1 and S2, respectively). These SEM and AFM results are in good agreement with the TEM observations.

To further understand the role of the block copolymers played in the cooperative self-assembly process, the effect of added water content on the aggregation behavior of graft copolymers and graft/block copolymer mixtures was studied. As shown in Figure 5a−c, for pure GP, TEM images reveal that with the addition of water, GP first self-assembled into cylinders, and then gradually transformed into vesicles. When the added water content reached 25 vol %, vesicles were exclusively achieved. For the mixtures, taking m_{BP2} = 0.5 for example, the cylinders are also obtained at a lower water content (5 vol %), as shown in Figure 5d. With increasing the water content, the aggregates maintain the cylindrical shape but the diameter increases (Figure 5e and 5f). With further increasing water content, the aggregate morphology does not change. These results indicate that for both pure graft copolymers and graft/block copolymer mixtures, cylinders are first formed at a lower water content. For pure graft copolymers, a cylinder-to-vesicle transition occurred with further increasing water content, while for the graft/block copolymer mixtures, the cylinders are stabilized by the block copolymers, which prevents the morphological transition (cylinder-to-vesicle) upon the further addition of water.

Aggregate Size and Structure Studied by LLS. The aggregate structure was further characterized by LLS. Figure 6a shows the hydrodynamic radius ($\langle R_h \rangle$) variation of the aggregates as a function of the mixture composition. For vesicles formed by pure GP and BP1, the $\langle R_h \rangle$ values are 197 and 170 nm, respectively. For GP/BP1 mixtures, with increasing m_{BP1}, the $\langle R_h \rangle$ value of aggregates first decreases to 150 nm around m_{BP1} = 0.25, and then slightly, but constantly increases. For GP/BP2 systems, the $\langle R_h \rangle$ value of the aggregates continually decreases from 197 to 132 nm with increasing m_{BP2} from 0 to 1.

The aggregate structure change can also be viewed in terms of the ratio of average radius of gyration ($\langle R_g \rangle$) to $\langle R_h \rangle$ ($\langle R_g \rangle / \langle R_h \rangle$), which is sensitive to the particle shape.[58,59] The $\langle R_g \rangle$ value of aggregates is calculated by extrapolating both the concentration and scattering angle to zero. A typical Berry plot of aggregates is shown in Figure S3 (see the Supporting Information). Generally, $\langle R_g \rangle / \langle R_h \rangle$ = 0.774 is regarded as a uniform and nondraining sphere. When $\langle R_g \rangle / \langle R_h \rangle$ = 1, it can be attributed to a vesicle geometry in theory. For nonspherical structures, $\langle R_g \rangle / \langle R_h \rangle$ usually has a large value. As shown in Figure 6b, the $\langle R_g \rangle / \langle R_h \rangle$ values of GP vesicles and BP1 vesicles are 1.09 and 1.01, respectively, which are very close to the ideal one. For GP/BP1 mixture aggregates, the $\langle R_g \rangle / \langle R_h \rangle$ values are larger than 1, which corresponds to the cylindrical structures. In addition, with increasing m_{BP1}, the $\langle R_g \rangle / \langle R_h \rangle$ value of aggregates increases first and reaches maximum value of ca. 1.50 around m_{BP1} = 0.25, and then continually decreases. Meanwhile, for the GP/BP2 aggregates, the change tendency of $\langle R_g \rangle / \langle R_h \rangle$ values is similar to that of GP/BP1 systems. In a word, the changes of $\langle R_g \rangle / \langle R_h \rangle$ value well correspond to the aggregate morphology transition of GP/BP mixtures observed from microscopies.

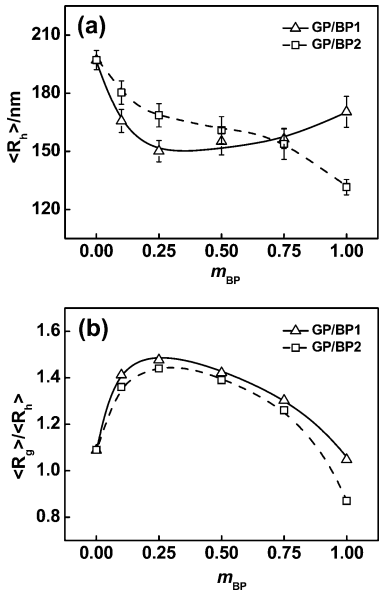

Figure 6. Plots of $\langle R_h \rangle$ (a), and $\langle R_g \rangle / \langle R_h \rangle$ (b) versus the weight fraction of block copolymers in the mixture systems.

SCFT Simulations. The above experiments reveal an interesting phenomenon that the mixtures of both vesicle-forming graft and block copolymers self-assemble into cylindrical micelles rather than vesicles. To understand such an experimental finding, we conducted an SCFT simulation on the system containing graft and block copolymers. The parameter was chosen according to the rule that both the graft and block copolymers can form vesicles. Therefore, such chosen parameters are not intended to represent the specific chemistry of PBLG-*g*-PEG/PBLG-*b*-PEG mixtures, but to capture the feature of the self-assembly behavior that both vesicle-forming graft and block copolymers can cooperatively aggregate into cylindrical micelles.

The simulation results for the aggregates formed by the mixtures of graft and block copolymers are presented in Figure 7. As shown in Figure 7a,b, pure graft and block copolymers self-assemble into vesicles. When a small volume fraction of the block copolymers is introduced into the graft copolymer solutions, e.g., ν_b = 0.25, the spherical and cylindrical micelles emerge, coexisting with the vesicles (Figure 7c). With further increasing ν_b to 0.5 or 0.75, the vesicles disappear, but spherical and cylindrical micelles are formed instead, as shown in Figure 7d,e. These simulation results reproduce the general feature of the morphological transition in vesicle-forming graft and block copolymer mixtures in experiments.

The simulation results can provide the detail information of chain distributions in the aggregates. Figure 8 shows the density distributions of the different components in various aggregates. The insets show the two-dimensional density profiles of the A and B blocks. The local volume fractions of hydrophobic A blocks in graft and block copolymers are ϕ_{A1} and ϕ_{A2},

dx.doi.org/10.1021/jp305956v | J. Phys. Chem. B 2012, 116, 10125−10134

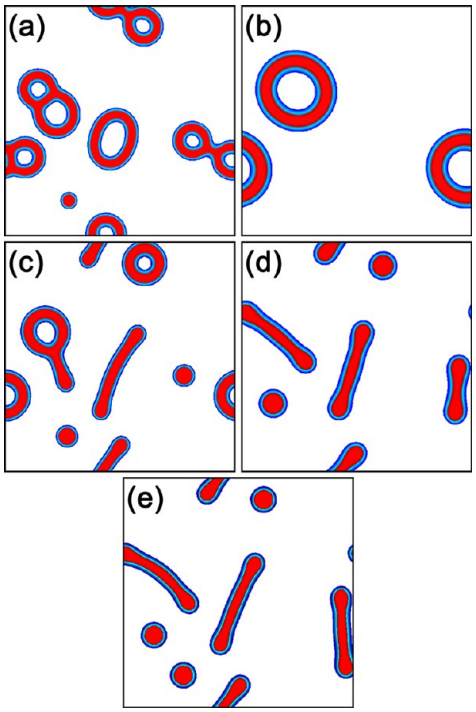

Figure 7. SCFT results of the aggregates self-assembled from the mixtures of the graft/block copolymers in dilute solution with the mixture contents of (a) $\nu_b = 0$, (b) $\nu_b = 1$, (c) $\nu_b = 0.25$, (d) $\nu_b = 0.5$, and (e) $\nu_b = 0.75$. The red and blue colors indicate regions rich in A and B blocks, respectively.

respectively (as represented by the red lines), while ϕ_{B1} and ϕ_{B2} are local volume fractions of hydrophilic B blocks in graft and block copolymers, respectively (as represented by the blue lines). In the vesicles respectively formed by pure graft and block copolymers, the density distributions have the similarity, as shown in Figure 8a,b. The distributions ϕ_{A1} and ϕ_{A2} exhibit a bimodal feature, which correspond to the vesicle geometry, that is, the hydrophobic A blocks form the vesicle walls, whereas the hydrophilic B blocks form the inner and outer leaves. This structural characteristic is consistent with various available observations.[56,60] While in the cylindrical micelles, the density distributions of graft and block copolymers show some differences. As displayed in Figure 8c, the profile of block copolymers (ϕ_{A2}) exhibits two remarkable peaks at the ends of the cylinders, implying that the block copolymers prefer to cap the cylindrical ends. Along the *Y*-direction of cylinders, however, the A block density profiles of both graft and block copolymers display nearly the same distributions, which means that the graft and block copolymers are mixed well in the micelle body (see Figure 8d). The above observations revealed the role of the block copolymers in the formation of cylindrical micelles, i.e., it prefers to cap the cylindrical ends.

It should be pointed out that, because of the inherent limitations, the SCFT simulations have difficulties in representing the rigid feature of the PBLG chain in the calculations. In addition to the solvophobic effect-induced PBLG chain aggregations, the strong interchain attraction (such as the strong dipolar $\pi-\pi$ interactions between the phenyl groups) and the volume exclusion effect could lead to orientational packing of the PBLG chain.[21,61−63] The PBLG chains could align with characteristics of liquid crystal structure.[37,39] Such packing in a liquid crystal manner could further lower the

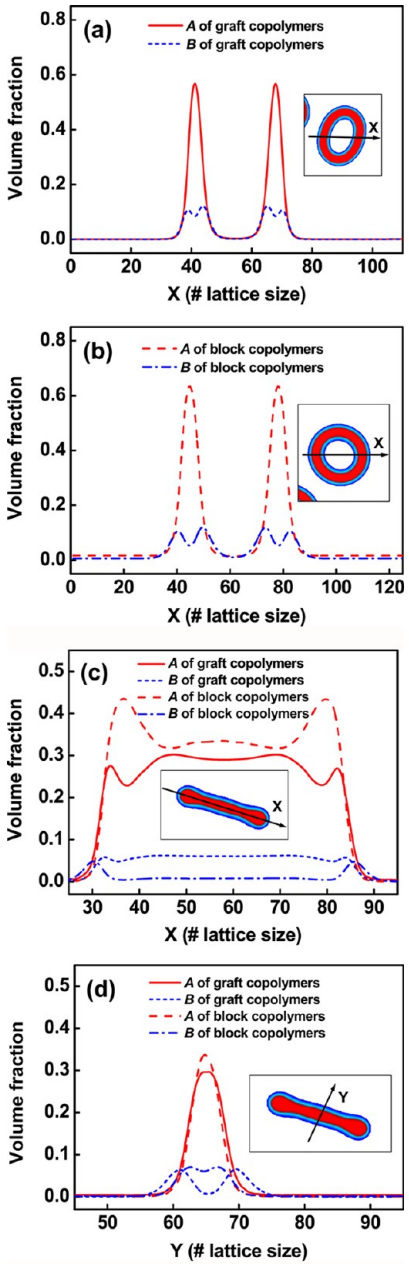

Figure 8. Density profiles of hydrophobic blocks ϕ_A and hydrophilic blocks ϕ_B of the aggregates marked with an arrow in the inset at various mixture contents: (a) $\nu_b = 0$, (b) $\nu_b = 1$, and (c, d) $\nu_b = 0.5$. The insets show the two-dimensional distribution of the hydrophobic A blocks (presented as red) and hydrophilic B blocks (presented as blue).

energy of the system. Although the SCFT simulations have difficulties in predicting the ordering of the molecular chains, the obtained results have provided meaningful information about the chain distribution, and are in favor of understanding the coassembly mechanism of the mixture system.

From the extensive experimental and SCFT results, we learned that PBLG-*b*-PEG block copolymers have marked influence on the self-assembly behavior of PBLG-*g*-PEG graft copolymers. Shown in Scheme 2 is a schematic illustration of morphological evolution of the PBLG-*g*-PEG/PBLG-*b*-PEG mixtures. For pure graft copolymers, with the addition of selective solvent (water), PBLG-*g*-PEG graft copolymers first self-assemble into cylindrical structures (Scheme 2a), in which

dx.doi.org/10.1021/jp305956v | J. Phys. Chem. B 2012, 116, 10125−10134

Scheme 2. Schematic Representation of the Morphological Transitions of PBLG-*g*-PEG/PBLG-*b*-PEG Copolymer Mixtures

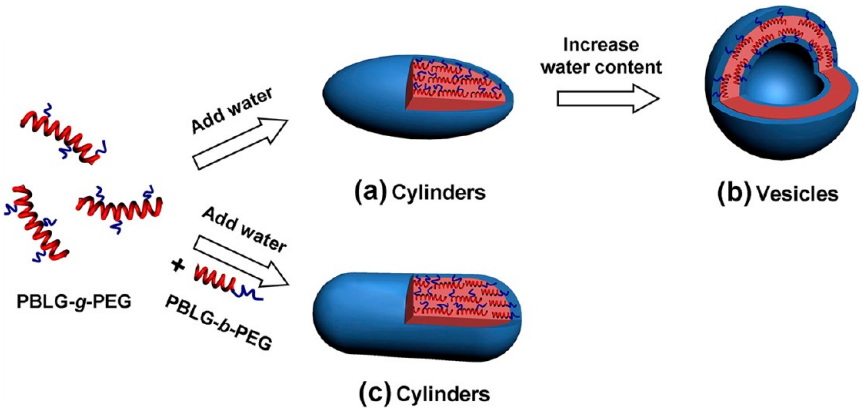

rigid PBLG backbones align with each other with their direction paralleled with the axial direction of the cylinders.[39] For the cylinders, the curvature in the ends is relative larger, thus the hydrophobic PBLG chains can not be effectively covered by short PEG chains. The unfavorable enthalpy between PBLG chains and water increases with increasing water content. Under this circumstance, the aggregates transform from the cylinders to closed structures such as vesicles (Scheme 2b), which possess a relative lower curvature with small interfacial area between PBLG wall and PEG chain.[2,3] In a vesicle wall, PBLG chains could slightly bend; however, considering the imperfect helix nature of the PBLG chains, the bended state of the PBLG chains in the wall of the vesicles can be achieved without raising the system energy markedly.[64,65] In addition, since the vesicles possess a very low curvature with smaller interfacial area between the PBLG wall and PEG chain, short PEG chains can shield the hydrophobic PBLG chains from being exposed to water effectively. As a result, stable vesicles are formed. In other words, the formation of stable vesicles is the interplay of enthalpic and entropic effects.

When PBLG-*b*-PEG block copolymers were introduced, cylindrical micelles were obtained (Figures 1 and 2). From the chain density distributions of the cylindrical micelles (Figure 8c,d), the block copolymers were found to be mainly distributed at the ends of cylinders. Combining with the experiment findings, it is believed that the block copolymers can cap the ends of the hybrid cylinders to shield the PBLG backbone of graft copolymers from being exposed to water. Meanwhile, the capping of block copolymers leads to an alleviation of the bending of PBLG chains (Scheme 2c). Thus, introducing the block copolymers into the graft copolymer system is in favor of the PBLG of graft copolymers in its preferential style, and results in aggregates with less frustrated chains.

Mixtures of amphiphilic copolymers provide attractive advantages over single-component formulations in achieving controllable and multifunctional properties, which will facilitate the applications of micelles in such fields as intelligent drug delivery systems. Meanwhile, a fundamental molecular level understanding of the coassembly of copolymer mixtures has significance for the complicated construction of cells, such as cell membranes, which are usually constructed from many different types of lipids. In the present work, we reported the cooperative self-assembly of mixture systems containing polypeptide-based graft and block copolymers. Such work provides information for insight into the self-assembly behavior of polypeptide-based copolymer mixtures. In addition, computer simulation on model systems can not only reproduce the experimental observations, but also provide microscopic information about the self-assembled aggregates, which could not be discerned using currently available experimental techniques. As the work presented, through the SCFT simulation predictions of density distributions of graft and block copolymers, the inherent structure of hybrid micelles and mechanism for the coassembly of mixture systems were obtained. The combination of computer simulation and experimental work facilitates the intensive investigation and deepens our understanding of complicated supramolecular systems.

■ CONCLUSIONS

The co-operative self-assembly behavior of mixture systems containing PBLG-*g*-PEG graft copolymers and PBLG-*b*-PEG block copolymers was studied by combining experimental methods and SCFT simulations. It was found that pure graft copolymers self-assembled into vesicles, and pure block copolymers formed spherical micelles or vesicles, while for the graft/block copolymer mixtures, cylindrical hybrid micelles were formed. For the cylinders, block copolymers were found to mainly locate at the ends of the cylinders, which prevents the fusion of primary self-assembled cylinders to vesicles. Overall, the results obtained from a combination of experiments and SCFT simulations are not only beneficial to understanding the formation of the vesicles from polypeptide-based graft copolymers, but also to enrich our knowledge of the self-assembly of multicomponent systems.

■ ASSOCIATED CONTENT

Supporting Information

SEM images of aggregate morphologies from mixture systems and so forth is available. This information is available free of charge via the Internet at http://pubs.acs.org.

■ AUTHOR INFORMATION

Corresponding Author

*Tel: +86-21-64253370; e-mail address: jlin@ecust.edu.cn.

Notes

The authors declare no competing financial interest.

■ ACKNOWLEDGMENTS

This work was supported by the National Natural Science Foundation of China (50925308), the Program for Changjiang Scholars and Innovative Research Team in University (No. IR T0825), and the National Basic Research Program of China (No. 2012CB933602). Support from projects of the Shanghai municipality (10GG115 and 08DZ2230500) is also appreciated.

■ REFERENCES

(1) Jain, S.; Bates, F. S. *Science* **2003**, *300*, 460−464.
(2) Gerard, R. *Prog. Polym. Sci.* **2003**, *28*, 1107−1170.
(3) Bhargava, P.; Tu, Y.; Zheng, J. X.; Xiong, H.; Quirk, R. P.; Cheng, S. Z. D. *J. Am. Chem. Soc.* **2007**, *129*, 1113−1121.
(4) Wang, X.; Guerin, G.; Wang, H.; Wang, Y.; Manners, I.; Winnik, M. A. *Science* **2007**, *317*, 644−647.
(5) Goswami, M.; Sumpter, B. G.; Huang, T. Z.; Messman, J. M.; Gido, S. P.; Isaacs-Sodeye, A. I.; Mays, J. W. *Soft Matter* **2010**, *6*, 6146−6154.
(6) Hadjichristidis, N.; Iatrou, H.; Pitsikalis, M.; Pispas, S.; Avgeropoulos, A. *Prog. Polym. Sci.* **2005**, *30*, 725−782.
(7) Liu, J.; Huang, W.; Pang, Y.; Zhu, X.; Zhou, Y.; Yan, D. *Biomaterials* **2010**, *31*, 5643−5651.
(8) van Dongen, S.; de Hoog, H.; Peters, R.; Nallani, M.; Nolte, R.; van Hest, J. *Chem. Rev.* **2009**, *109*, 6212−6274.
(9) Zheng, R.; Liu, G.; Yan, X. *J. Am. Chem. Soc.* **2005**, *127*, 15358−15359.
(10) Bull, S. R.; Palmer, L. C.; Fry, N. J.; Greenfield, M. A.; Messmore, B. W.; Meade, T. J.; Stupp, S. I. *J. Am. Chem. Soc.* **2008**, *130*, 2742−2743.
(11) Schacher, F.; Betthausen, E.; Walther, A.; Schmalz, H.; Pergushov, D. V.; Muller, A. H. E. *ACS Nano* **2009**, *3*, 2095−2102.
(12) Luo, L.; Eisenberg, A. *Angew. Chem., Int. Ed.* **2002**, *41*, 1001−1004.
(13) Hui, T.; Chen, D.; Jiang, M. *Macromolecules* **2005**, *38*, 5834−5837.
(14) Hu, J.; Liu, G. *Macromolecules* **2005**, *38*, 8058−8065.
(15) Li, G.; Shi, L.; Ma, R.; An, Y.; Huang, N. *Angew. Chem., Int. Ed.* **2006**, *45*, 4959−4962.
(16) Davis, K. P.; Lodge, T. P.; Bates, F. S. *Macromolecules* **2008**, *41*, 8289−8291.
(17) Wan, S.; Jiang, M.; Zhang, G. *Macromolecules* **2007**, *40*, 5552−5558.
(18) Ma, L.; Liu, R.; Tan, J.; Wang, D.; Jin, X.; Kang, H.; Wu, M.; Huang, Y. *Langmuir* **2010**, *26*, 8697−8703.
(19) Li, Y.; Zhang, Y.; Yang, D.; Li, Y.; Hu, J.; Feng, C.; Zhai, S.; Lu, G.; Huang, X. *Macromolecules* **2009**, *43*, 262−270.
(20) Li, Z.; Kesselman, E.; Talmon, Y.; Hillmyer, M. A.; Lodge, T. P. *Science* **2004**, *306*, 98−101.
(21) Junnila, S.; Houbenov, N.; Hanski, S.; Iatrou, H.; Hirao, A.; Hadjichristidis, N.; Ikkala, O. *Macromolecules* **2010**, *43*, 9071−9076.
(22) Rao, J.; Zhang, Y.; Zhang, J.; Liu, S. *Biomacromolecules* **2008**, *9*, 2586−2593.
(23) Lo, C.-L.; Huang, C.-K.; Lin, K.-M.; Hsiue, G.-H. *Biomaterials* **2007**, *28*, 1225−1235.
(24) Ouarti, N.; Viville, P.; Lazzaroni, R.; Minatti, E.; Schappacher, M.; Deffieux, A.; Putaux, J. L.; Borsali, R. *Langmuir* **2005**, *21*, 9085−9090.
(25) Li, Z.; Hillmyer, M. A.; Lodge, T. P. *Macromolecules* **2006**, *39*, 765−771.
(26) Feng, C.; Li, Y.; Yang, D.; Hu, J.; Zhang, X.; Huang, X. *Chem. Soc. Rev.* **2011**, *40*, 1282−1295.
(27) Kotharangannagari, V. K.; Sanchez-Ferrer, A.; Ruokolainen, J.; Mezzenga, R. *Macromolecules* **2011**, *44*, 4569−4573.
(28) He, C.; Zhao, C.; Guo, X.; Guo, Z.; Chen, X.; Zhuang, X.; Liu, S.; Jing, X. *J. Polym. Sci., Part A: Polym. Chem.* **2008**, *46*, 4140−4150.
(29) Zhao, J.; Mountrichas, G.; Zhang, G.; Pispas, S. *Macromolecules* **2010**, *43*, 1771−1777.
(30) Carlsen, A.; Lecommandoux, S. *Curr. Opin. Colloid Interface Sci.* **2009**, *14*, 329−339.
(31) Rodriguez-Hernandez, J.; Lecommandoux, S. *J. Am. Chem. Soc.* **2005**, *127*, 2026−2027.
(32) Rao, J.; Luo, Z.; Ge, Z.; Liu, H.; Liu, S. *Biomacromolecules* **2007**, *8*, 3871−3878.
(33) Iatrou, H.; Frielinghaus, H.; Hanski, S.; Ferderigos, N.; Ruokolainen, J.; Ikkala, O.; Richter, D.; Mays, J.; Hadjichristidis, N. *Biomacromolecules* **2007**, *8*, 2173−2181.
(34) Cai, C.; Wang, L.; Lin, J. *Chem. Commun.* **2011**, *47*, 11189−11203.
(35) Li, Z.; Deming, T. J. *Soft Matter* **2010**, *6*, 2546−2551.
(36) Luo, K.; Yin, J.; Song, Z.; Cui, L.; Cao, B.; Chen, X. *Biomacromolecules* **2008**, *9*, 2653−2661.
(37) Cai, C.; Lin, J.; Chen, T.; Wang, X.; Lin, S. *Chem. Commun.* **2009**, 2709−2711.
(38) Lin, J.; Zhu, J.; Chen, T.; Lin, S.; Cai, C.; Zhang, L.; Zhuang, Y.; Wang, X. S. *Biomaterials* **2009**, *30*, 108−117.
(39) Cai, C.; Lin, J.; Chen, T.; Tian, X. *Langmuir* **2010**, *26*, 2791−2797.
(40) Li, T.; Lin, J.; Chen, T.; Zhang, S. *Polymer* **2006**, *47*, 4485−4489.
(41) Tang, D.; Lin, J.; Lin, S.; Zhang, S.; Chen, T.; Tian, X. *Macromol. Rapid Commun.* **2004**, *25*, 1241−1246.
(42) Zhang, L.; Lin, J.; Lin, S. *Macromolecules* **2007**, *40*, 5582−5592.
(43) Zhu, X.; Wang, L.; Lin, J.; Zhang, L. *ACS Nano* **2010**, *4*, 4979−4988.
(44) Jiang, Y.; Chen, T.; Ye, F.; Liang, H.; Shi, A.-C. *Macromolecules* **2005**, *38*, 6710−6717.
(45) Xia, Y.; Chen, J.; Sun, Z.; Shi, T.; An, L.; Jia, Y. *Polymer* **2010**, *51*, 3315−3319.
(46) Ma, Z.; Yu, H.; Jiang, W. *J. Phys. Chem. B* **2009**, *113*, 3333−3338.
(47) Cai, C.; Zhang, L.; Lin, J.; Wang, L. *J. Phys. Chem. B* **2008**, *112*, 12666−12673.
(48) Han, Y.; Yu, H.; Du, H.; Jiang, W. *J. Am. Chem. Soc.* **2009**, *132*, 1144−1150.
(49) Ma, J.; Li, X.; Tang, P.; Yang, Y. *J. Phys. Chem. B* **2007**, *111*, 1552−1558.
(50) Zhuang, Y.; Lin, J.; Wang, L.; Zhang, L. *J. Phys. Chem. B* **2009**, *113*, 1906−1913.
(51) Xu, G.; Feng, X.; Li, Y. *J. Phys. Chem. B* **2010**, *114*, 1257−1263.
(52) Blout, E. R.; Karlson, R. H. *J. Am. Chem. Soc.* **1956**, *78*, 941−946.
(53) Cai, C.; Zhu, W.; Chen, T.; Lin, J.; Tian, X. *J. Polym. Sci., Part A: Polym. Chem.* **2009**, *47*, 5967−5978.
(54) Inomata, K.; Ohara, N.; Shimizu, H.; Nose, T. *Polymer* **1998**, *39*, 3379−3386.
(55) Li, X.; Tang, P.; Qiu, F.; Zhang, H.; Yang, Y. *J. Phys. Chem. B* **2006**, *110*, 2024−2030.
(56) Zhang, L.; Lin, J.; Lin, S. *J. Phys. Chem. B* **2007**, *111*, 9209−9217.
(57) Sun, J.; Chen, X.; Deng, C.; Yu, H.; Xie, Z.; Jing, X. *Langmuir* **2007**, *23*, 8308−8315.
(58) Vagberg, L. J. M.; Cogan, K. A.; Gast, A. P. *Macromolecules* **1991**, *24*, 1670−1677.
(59) Wu, C.; Li, M.; Kwan, S. C. M.; Liu, G. J. *Macromolecules* **1998**, *31*, 7553−7554.
(60) Wang, R.; Tang, P.; Qiu, F.; Yang, Y. *J. Phys. Chem. B* **2005**, *109*, 17120−17127.
(61) Minich, E. A.; Nowak, A. P.; Deming, T. J.; Pochan, D. J. *Polymer* **2004**, *45*, 1951−1957.
(62) Kim, K. T.; Park, C.; Vandermeulen, G. W. M.; Rider, D. A.; Kim, C.; Winnik, M. A.; Manners, I. *Angew. Chem., Int. Ed.* **2005**, *44*, 7964−7968.
(63) Uematsu, I.; Uematsu, Y. *Adv. Polym. Sci.* **1984**, *59*, 37−73.
(64) Floudas, G.; Spiess, H. W. *Macromol. Rapid Commun.* **2009**, *30*, 278−298.

(65) Papadopoulos, P.; Floudas, G.; Klok, H. A.; Schnell, I.; Pakula, T. *Biomacromolecules* **2004**, *5*, 81−91.